Ultrasound-Assisted Control of Porosity Distribution in Adhesive and Resin Systems for Composite Manufacturing

D. Csehngeri[1*], A. Poursartip[2], and E. Cretu[1]

[1] Department of Electrical & Computer Engineering, University of British Columbia, 5500 – 2332 Main Mall, Vancouver, V6T 1Z4, British Columbia, Canada, [2] Composites Research Network, Materials Engineering, University of British Columbia, 309-6350 Stores Road, Vancouver, V6T 1Z4, British Columbia, Canada

* *Corresponding author (daniel.csehngeri@ubc.ca)*

Keywords: *polymer processing, porosity control, ultrasound processing, epoxy resin*

1. Abstract

Epoxy resins are widely used as structural adhesives and as matrix materials for carbon fiber reinforced polymers (CFRP) in aerospace and automotive manufacturing. Their curing processes, however, are highly sensitive to processing conditions. Entrapped air and voids commonly form during manufacturing, both within fiber tows and at the fiber-matrix interface, and cannot be fully eliminated even under controlled industrial conditions. While some porosity may be tolerable depending on its size and location, uncontrolled defect formation can adversely affect mechanical performance and process reliability. Although ultrasound has been applied to resin degassing, the controlled manipulation of porosity during composite processing remains largely unexplored.

The objective of this work is to assess the feasibility of using ultrasonic energy to actively influence the motion of air inclusions in liquid resin systems as a potential tool for porosity control in early stages of cure. Several types of ultrasonic actuators, for example commercial piezoelectric ultrasonic transducers and polymer-based capacitive micromachined ultrasonic transducers (polyCMUTs) were investigated. Key parameters, including ultrasonic frequency, applied acoustic power, and excitation duration, were systematically varied to evaluate their influence on porosity displacement.

All transducers were first characterized in a water bath using a calibrated hydrophone to determine their acoustic output and operating characteristics. For controlled visualization experiments, epoxy resin was substituted with silicone oil possessing comparable acoustic properties. The fluid was contained in a high-density polyethylene (HDPE) mold, and air inclusions with diameters of up to 5 mm were introduced in a reproducible manner. Ultrasonic energy was applied through the mold wall at mechanical power levels of up to 7 W, and bubble motion was monitored optically.

Preliminary results demonstrate that ultrasonic excitation can induce directed movement of air inclusions, with observed velocities on the order of several centimeters per second under specific operating conditions. These proof-of-concept findings indicate that ultrasound has the potential to reshape porosity distribution prior to gelation, offering a possible pathway toward improved process control in CFRP manufacturing.

2. Introduction

Conventional mechanical joining methods, such as riveting and bolting, present several inherent disadvantages, including the introduction of stress concentrations and additional structural weight [1]. Adhesive bonding offers a compelling alternative, enabling uniform stress distribution, the joining of dissimilar materials, and greater design flexibility. As a result, it is widely employed in aerospace, automotive, and other high-performance engineering applications using a variety of adhesive systems, including epoxies, silicones, and polyurethanes. Despite these advantages, adhesive bonding remains highly sensitive to processing conditions and is associated with several challenges, including insufficient surface wetting, surface contamination, incomplete curing, and the formation of porosity within the bond line [2]. Proper surface preparation is therefore critical, with surface roughness playing a key role in promoting mechanical interlocking and adhesion [3]. To ensure adequate bonding, a range of surface treatment techniques are employed, from mechanical abrasion to advanced methods such as plasma treatment. Additionally, environmental factors such as moisture can significantly degrade joint performance and long-term durability [4].

Among these challenges, porosity and void formation represent some of the most critical defects in adhesively bonded joints. Entrapped air during mixing and application, as well as volatiles generated during curing, lead to the formation of micro-voids within the adhesive layer [2,5]. These defects reduce the effective load-bearing cross-section and act as stress concentrators, thereby degrading the mechanical performance of the joint [6]. In research, they can be simulated with porous PTFE films [7] or by introducing metal shims between both adherends to artificially increase bond line thickness [8]. Experimental studies have consistently shown that increasing void content leads to reductions in tensile strength, fracture toughness, and fatigue resistance of adhesive systems [8,9]. For example, Costa et al. [10] have shown decreases in shear strength of 35% at a porosity of ~5%. In addition to the overall void fraction, the size, morphology, and spatial distribution of voids can be equally important in determining failure behavior, as localized defect concentrations promote premature crack initiation and can shift damage zones within the adhesive layer [11]. Moreover, porosity is difficult to eliminate entirely under practical manufacturing conditions and is therefore commonly present in structural adhesive bonds [12].

Given the detrimental impact of porosity on joint performance, approaches that enable active control of void motion and distribution are of significant interest. Acoustic methods, in particular, offer a potential pathway for such control. Acoustic levitation and particle manipulation using ultrasonic fields are well-established concepts, widely studied in the context of acoustofluidics [13,14]. Ultrasound has been used to actuate impurities in fluids, ranging from simple degassing to the controlled manipulation of microscopic particles using acoustic tweezers [15,16]. These effects arise from acoustic radiation forces acting on inclusions with acoustic property contrasts relative to the surrounding fluid, including both solid particles and gas bubbles, enabling their directed motion within pressure fields. For example, Dai et al. [16] demonstrated particle separation using a phased ultrasonic array, while other studies have achieved precise micro-particle and bubble manipulation using tunable ultrasonic bottle beams without requiring phased arrays [17].

Acoustic forces have also been investigated in the context of polymer processing and composite manufacturing. At low to moderate excitation levels, where cavitation is negligible, ultrasonic fields can influence resin flow, filler dispersion, and inclusion motion through acoustic radiation forces [18]. Furthermore, their effect on cure acceleration has been reported at frequencies on the order of 40 kHz under appropriate acoustic conditions [19]. In composite manufacturing processes, ultrasound has been applied to study void formation and suppression during resin transfer molding (RTM) [20]. In contrast, at high power levels, such as electrical input levels approaching 1800 W, cavitation effects dominate, leading to bubble oscillation, collapse, and potentially uncontrolled agglomeration or displacement of porosity [21]. Furthermore, in ultrasonic-assisted bonding, the application of acoustic energy during joint formation has been shown to significantly increase shear strength by enhancing surface wetting and mechanical interlocking [22].

Despite these advances, the controlled manipulation of porosity during adhesive bonding and composite curing remains largely unexplored. Existing studies either focus on bulk material effects, such as enhanced curing or dispersion, or rely on high-power, cavitation-dominated regimes that are difficult to control and may not be suitable for sensitive manufacturing processes. While precise acoustic manipulation of particles and bubbles has been demonstrated in low-viscosity fluids using techniques such as phased arrays or structured acoustic fields, these approaches have not been translated to viscous, curing thermoset systems relevant to adhesive bonding or composite manufacturing. As a result, there is currently no established approach for the controlled, directional redistribution of porosity within adhesive bond lines or resin systems under industrially relevant conditions.

This study demonstrates the directional displacement of porosity in liquid resin systems using low-power ultrasonic excitation, with electrical input levels well below 50 W. The influence of key parameters, including excitation frequency and transducer type, is systematically investigated. Different transducer technologies are evaluated with respect to their suitability for acoustic actuation in viscous resin systems. The results provide proof-of-concept evidence that ultrasonic excitation above a certain threshold can induce preferential redistribution of porosity prior to gelation, demonstrating the potential for spatial control of defect distribution and offering a pathway toward improved process reliability in adhesive bonding and composite manufacturing.

3. Methodology

The experimental setup was designed to approximate conditions relevant to adhesive bonding and composite manufacturing processes, while maintaining a high degree of experimental control and repeatability. All experiments were conducted using an identical configuration. A custom mold fabricated from high-density polyethylene (HDPE) with planar dimensions of 300 × 300 mm and a thickness of 3.5 mm was used. The material was selected for its favorable acoustic properties and relatively low acoustic impedance mismatch with the test fluid. A fluid layer of 4 mm thickness was introduced into the mold.

Instead of a thermosetting epoxy resin, silicone oil was employed as a model fluid to avoid complications associated with curing during extended experimental runs (XIAMETER™ PMX200, 100 cSt). This fluid has been widely used as a surrogate in composite curing studies [23] due to its well-characterized properties and suitable viscosity range, which is comparable to various epoxies used for resin infusion processes at ~0.1Pa*s. The mold was mounted on four aluminum T-slot support structures to ensure sufficient separation from the workbench and to minimize unintended acoustic coupling, as can be seen in Figure 1.

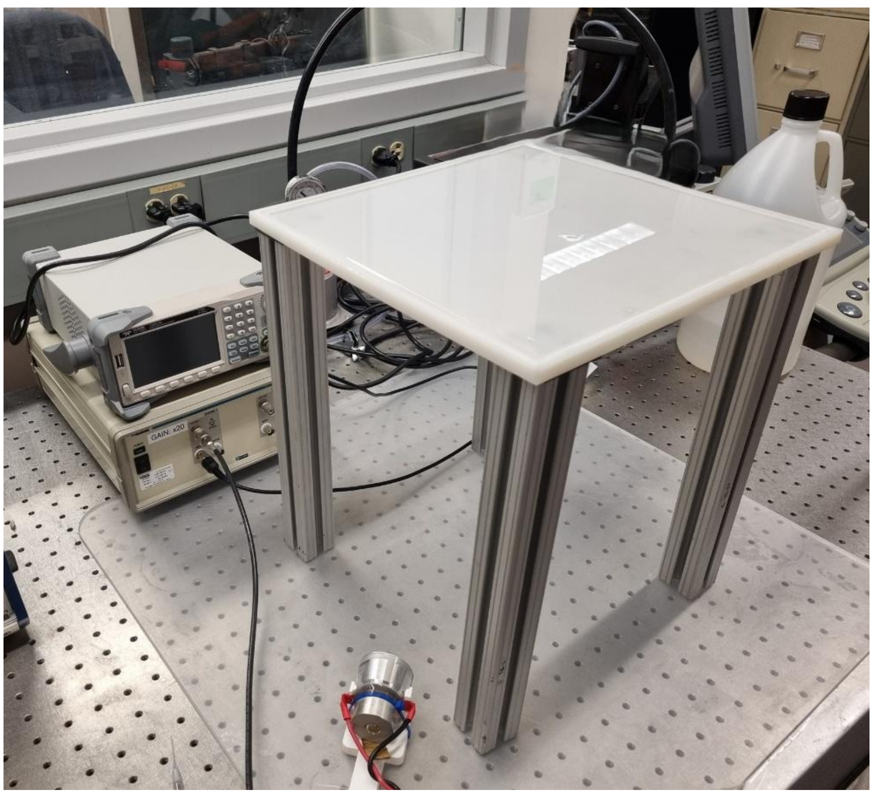

Figure 1: Experimental Setup

The mold was sealed with a transparent polymethyl methacrylate lid (PMMA) to allow optical access during experiments. To ensure a controlled initial condition, the system was first degassed to remove pre-existing air inclusions. A small aperture in the lid enabled the controlled introduction of individual air bubbles using a syringe, allowing adjustment of bubble size and initial position. The generated bubbles had typical diameters on the order of 2 mm and were located near the upper boundary of the fluid due to buoyancy. All experiments were conducted at room temperature (approximately 21 °C).

Ultrasonic excitation was applied using three different transducer types to cover a broad range of frequencies and operating characteristics. A commercial piezoelectric transducer (NBL45402H-A, Yageo, Taiwan) with a nominal center frequency of 40 kHz and an aperture of 45mm diameter was used to represent low-frequency operation typical of ultrasonic cleaning systems. In addition, a custom-built single-crystal piezoelectric transducer with an operating range from approximately 1.2 to 3.5 MHz and an aperture of 20mm diameter was employed, as well as a polymer-based capacitive micromachined ultrasonic transducer (polyCMUT) with a center frequency of approximately 1 MHz and an array diameter of ~10mm. This range of transducers enables investigation of frequency-dependent effects on bubble dynamics and displacement behavior.

All transducers were driven by a function generator producing a continuous sinusoidal signal at the desired frequency and amplitude. The signal was amplified using a high-voltage amplifier (gain ×20) prior to excitation of the transducer. The excitation voltage at the function generator was varied between 1 and 10 Vpp, corresponding to amplified voltage levels of approximately 20 to 200 Vpp at the transducer. This applied voltage range enables comparative assessment of excitation thresholds across different transducer configurations.

The transducer was positioned beneath the mold, with acoustic coupling ensured through the application of ultrasonic gel at the interface. The generated acoustic waves propagated through the mold and fluid layer, establishing an acoustic pressure field within the silicone oil.

Each experimental condition was applied for a duration of approximately 3 minutes to allow sufficient time for observable bubble response. Bubble motion was monitored optically through the transparent lid and recorded using a digital camera for qualitative analysis.

4. Results: Transducer-Dependent Porosity Manipulation

4.1. NBL45402H-A (40 kHz center frequency)

A baseline study was first performed using the NBL45402H-A transducer, operating at its center frequency of 40 kHz. A single gas bubble with an approximate diameter of 2 mm was introduced into the silicone oil via a controlled injection port in the mould lid. The transducer was driven using a continuous sinusoidal excitation at 40 kHz. The input signal from the function generator was amplified to achieve output voltages ranging from 60 Vpp to 200 Vpp (approximately 21.2 Vrms to 70.7 Vrms).

Hydrophone-based calibration of the acoustic field established an approximately linear relationship between applied drive voltage and acoustic pressure amplitude, with a measured sensitivity of approximately 180 Pa/Vrms. This calibration was used to estimate the corresponding acoustic pressure levels during operation.

At a drive level of approximately 21.2 Vrms (~60 Vpp), the resulting acoustic pressure amplitude was on the order of ~3.8 kPa. Under these conditions, bubble motion was clearly observable, and the bubble could be displaced controllably through the resin at velocities of several millimeters per second. When the excitation amplitude was increased to approximately 70.7 Vrms (~200 Vpp), the estimated acoustic pressure amplitude increased to approximately ~13 kPa. Under these conditions, bubble manipulation became significantly easier, and controlled displacement over several centimeters per second was possible, as seen in Figure 2. During motion, the bubble exhibited pronounced deformation.

Figure 2: Temporal Evolution of Bubble Movement Due to Ultrasound. From Top Left to Bottom Right: t= 0, 2, 4, 6s.

4.2. Custom-Built Piezoelectric Transducer (MHz-Range Operation)

A custom-built piezoelectric transducer was subsequently evaluated to investigate bubble response under high-frequency excitation conditions. To ensure comparability with the previously tested system and to remain within a safe operating range, the excitation amplitude was limited to a maximum of 60 Vpp. The device exhibited a broadband frequency response over approximately 1.2 MHz to 3.5 MHz. Bubble response was therefore evaluated across this frequency range. Across all tested frequencies, a qualitatively similar response was observed, characterized by localized oscillatory motion rather than sustained translational displacement. The most pronounced oscillation occurred near ~1.8 MHz, corresponding to the resonance region of the transducer. At this frequency, bubble oscillation amplitude was maximized; however, no stable directional transport could be achieved. The bubble exhibited small-amplitude oscillatory motion (“wriggling”) about its equilibrium position, without measurable net displacement through the resin.

4.3. polyCMUT

Finally, a polymer-based capacitive micromachined ultrasonic transducer (polyCMUT) was evaluated as a third excitation source. This transducer design offers advantages such as wide operational bandwidth, array-based configurability, and simplified fabrication compared to conventional piezoelectric systems [24]. However, these benefits are typically associated with lower maximum achievable acoustic output levels. To maximize actuation, the device was operated at its maximum allowable excitation level of 20 Vpp. A driving frequency of 1 MHz was selected, corresponding to the nominal center frequency of the transducer. Under these conditions, no observable bubble motion was detected. The bubble remained stationary, with no measurable translational displacement or oscillatory response.

5. Discussion

5.1. Regimes of Bubble Behaviour

The experimental results reveal three distinct regimes of bubble behavior as a function of the applied acoustic excitation. For the polyCMUT transducer, no observable bubble motion was detected, indicating that the applied acoustic forcing remained below the threshold required to induce a measurable response. The custom-built MHz-range piezoelectric transducer produced localized oscillatory motion of the bubble without sustained translational displacement. In contrast, the 40 kHz piezoelectric transducer enabled controlled bubble transport through the resin, with displacement velocities increasing with excitation amplitude. These observations indicate the presence of a threshold-dependent transition between non-responsive, oscillatory, and transport regimes. The existence of such a threshold is consistent with the need to overcome viscous resistance and interfacial restoring forces in the viscous fluid system.

5.2. Governing Parameters and Effective Actuation Strength

While acoustic pressure amplitude provides a useful first-order metric for describing operating conditions, it does not fully capture the observed differences in bubble mobility across transducers. Experimental results demonstrate that comparable pressure levels do not necessarily result in similar bubble responses. This indicates that bubble motion is governed by a combination of acoustic field characteristics, including:

- acoustic pressure amplitude

- spatial pressure gradients
- oscillatory particle velocity fields, particularly in the acoustic near field
- effective mechanical coupling into the medium

Despite similar electrical input levels, the low-frequency transducer exhibited significantly greater effectiveness in inducing bubble transport. This behavior is attributed to its stronger physical displacement amplitude, resulting in higher induced particle velocity amplitudes and more pronounced acoustic forcing. In contrast, the MHz-range transducer produced only localized oscillatory motion, while the polyCMUT system did not reach the threshold required to initiate any observable bubble response. These findings indicate that the ability to induce translational motion depends on exceeding a critical level of effective forcing associated with hydrodynamic drag and fluid motion, rather than on excitation frequency or acoustic pressure amplitude alone.

5.3. Mechanisms of Bubble Motion

The observed bubble dynamics are attributed to a combination of acoustic radiation forces and acoustically induced fluid motion. Acoustic radiation forces arise from the strong acoustic impedance mismatch between the gas bubble and the surrounding fluid, generating net forces in regions of spatial pressure gradients. However, the pronounced bubble transport observed under low-frequency, high-displacement excitation strongly suggests a dominant contribution from acoustically induced fluid motion. In particular, acoustic streaming generated by large oscillatory surface velocities is expected to produce steady flow fields capable of entraining and transporting bubbles over extended distances. Acoustic streaming may therefore play a central role in bubble transport, particularly in the low-viscosity regime prior to gelation. The relative contributions of radiation forces and streaming are expected to depend on the acoustic field structure, excitation amplitude, and the rheological state of the resin.

5.4. Limitations and Implications for Process Design

Several limitations of the present study should be noted. No direct measurements of particle velocity fields, acoustic streaming, or transducer surface displacement were performed. Bubble size was not systematically varied, and the analysis is based primarily on qualitative observations of bubble motion. While these limitations restrict quantitative interpretation, they do not affect the identification of the observed behavioural regimes and underlying trends.

The results demonstrate that effective bubble manipulation in curing thermoset systems requires exceeding a threshold in acoustic actuation strength. This threshold is expected to depend on both the rheological state of the resin and the characteristic size of the bubbles. From a practical perspective, low-frequency, high-displacement transducers appear more suitable for inducing controlled bubble transport in viscous media under comparable electrical input conditions. In contrast, high-frequency systems may be more effective for inducing localized oscillatory effects rather than bulk transport. These findings provide a basis for the design of ultrasound-assisted processes aimed at porosity control in composite manufacturing, where both the spatial redistribution and potential fragmentation of bubbles may be exploited.

6. Conclusion

This study investigated ultrasound-assisted manipulation of gas inclusions in a curing epoxy system, approximated with silicone oil, using three fundamentally different ultrasonic transducers operating across a wide frequency and actuation range. The primary objective was to assess whether acoustic fields can induce controlled redistribution of bubbles during the early stages of thermoset curing, and to identify the governing parameters for bubble mobility in a highly viscous, evolving medium. This work demonstrates that bubble mobility in curing thermoset systems is governed by a threshold in effective acoustic actuation strength, rather than excitation frequency alone, and identifies distinct regimes of non-response, oscillatory motion, and controlled transport.

Experiments using an 40 kHz piezoelectric transducer demonstrated robust bubble manipulation within the resin. At sufficient excitation levels, bubbles could be displaced controllably at millimeter-per-second to centimeter-per-second scales. Hydrophone-based calibration confirmed that bubble mobility increased with acoustic pressure amplitude; however, comparative analysis across transducers indicated that pressure alone is not sufficient to describe actuation efficiency.

A custom-built MHz-range piezoelectric transducer exhibited a markedly different response. Despite operation near its resonance frequency (~1.8 MHz), bubble motion was limited to localized oscillatory behavior without sustained translational transport. This suggests a transition from a transport-dominated regime to a localized deformation regime, governed primarily by a reduced physical displacement amplitude of the transducer and coupling efficiency rather than frequency alone.

A third transducer based on a polymer CMUT architecture produced no observable bubble motion under maximum available excitation (20 Vpp at 1 MHz). This result defines a lower bound for acoustic actuation in the present system and supports the existence of a threshold in effective acoustic forcing required to overcome viscous resistance and interfacial restoring forces within the partially curing resin.

Across all configurations, the results indicate that bubble mobility in a viscous fluid is governed by a combination of acoustic pressure amplitude, spatial field gradients, and effective mechanical coupling into the medium. In particular, bubble transport appears to be controlled by a threshold-dependent transition between non-mobility, oscillatory response, and net translational motion. These findings suggest that acoustic streaming and radiation force-driven transport mechanisms are likely to be active across a broad frequency range, but their effectiveness strongly depends on the achievable acoustic actuation strength and the resulting field structure rather than the excitation frequency alone. From an application perspective, the results highlight the need to define optimal actuation parameters based on the rheological state of the resin and the characteristic bubble size distribution. In particular, viscosity evolution during curing is expected to strongly influence the onset threshold for bubble mobility.

Future work should therefore focus on numerical modeling of coupled acoustic–bubble–viscoelastic interactions, for example using multiphysics simulation frameworks such as COMSOL, to predict bubble trajectories under time-evolving material properties. Finally, the observed tendency for bubbles to undergo deformation and partial fragmentation under strong acoustic excitation suggests a potential secondary application: ultrasound-assisted reduction of bubble size distributions. This could enable not only bubble removal or transport, but also controlled refinement of porosity structures during composite manufacturing.

7. References

[1] Omairey, S. *et al.* (2021). Defects and uncertainties of adhesively bonded composite joints. *SN Applied Sciences*. https://doi.org/10.1007/s42452-021-04753-8.

[2] Dachev, D. *et al.* (2025). Towards Reliable Adhesive Bonding: A Comprehensive Review of Mechanisms, Defects, and Design Considerations. *Materials*. https://doi.org/10.3390/ma18122724.

[3] Zhang, D. and Huang, Y. (2021). Influence of surface roughness and bondline thickness on the bonding performance of epoxy adhesive joints on mild steel substrates. *Progress in Organic Coatings*. https://doi.org/10.1016/j.porgcoat.2021.106135.

[4] Ogata, S. and Uranagase, M. (2018). Unveiling the Chemical Reactions Involved in Moisture-Induced Weakening of Adhesion between Aluminum and Epoxy Resin. *The Journal of Physical Chemistry C*. https://doi.org/10.1021/acs.jpcc.8b03549.

[5] Katnam, K.B. *et al.* (2011). Tensile strength of two-part epoxy paste adhesives: Influence of mixing technique and micro-void formation. *International Journal of Adhesion and Adhesives*. https://doi.org/10.1016/j.ijadhadh.2011.06.005.

[6] Dumont, V. *et al.* (2020). On the influence of mechanical loadings on the porosities of structural epoxy adhesives joints by means of in-situ X-ray microtomography. *International Journal of Adhesion and Adhesives*. https://doi.org/10.1016/j.ijadhadh.2020.102568.

[7] Zhang, T. *et al.* (2019). The influence of adhesive porosity on composite joints. *Composites Communications*. https://doi.org/10.1016/j.coco.2019.06.011.

[8] Guin, W.E. *et al.* (2025). Characterization of fracture behavior in adhesively bonded joints with porosity in the adhesive layer using X-ray computed tomography. *Composites Science and Technology*. https://doi.org/10.1016/j.compscitech.2024.111025.

[9] Fernandez, G. *et al.* (2018). Static and cyclic strength properties of brittle adhesives with porosity. *International Journal of Fatigue*. https://doi.org/10.1016/j.ijfatigue.2018.08.018.

[10] Costa, M.L. *et al.* (2001). The influence of porosity on the interlaminar shear strength of carbon/epoxy and carbon/bismaleimide fabric laminates. *Composites Science and Technology*. https://doi.org/10.1016/S0266-3538(01)00157-9.

[11] Fan, J. *et al.* (2024). Void content and displacement ratio effects on fatigue crack growth in thick adhesively bonded composite joints under constant amplitude loading. *International Journal of Fatigue*. https://doi.org/10.1016/j.ijfatigue.2024.108508.

[12] Marzo, A. *et al.* (2015). Holographic acoustic elements for manipulation of levitated objects. *Nature Communications*. https://doi.org/10.1038/ncomms9661.

[13] Zang, D. (ed.) (2020). *Acoustic Levitation: From Physics to Applications*, Springer Singapore, Singapore.

[14] Friend, J. and Yeo, L.Y. (2011). Microscale acoustofluidics: Microfluidics driven via acoustics and ultrasonics. *Reviews of Modern Physics*. https://doi.org/10.1103/RevModPhys.83.647.

[15] Ozcelik, A. *et al.* (2018). Acoustic tweezers for the life sciences. *Nature Methods*. https://doi.org/10.1038/s41592-018-0222-9.

[16] Dai, H. *et al.* (2025). Acoustic manipulation for particles motion transformation by ultrasonic phased arrays. *Sensors and Actuators A: Physical*. https://doi.org/10.1016/j.sna.2025.116700.

[17] Zhou, Q. *et al.* (2021). Precise micro-particle and bubble manipulation by tunable ultrasonic bottle beams. *Ultrasonics Sonochemistry*. https://doi.org/10.1016/j.ultsonch.2021.105602.

[18] Uribe, B. *et al.* (2024). Application of Sound Waves During the Curing of an Acrylic Resin and Its Composites Based on Short Carbon Fibers and Carbon Nanofibers. *Materials*. https://doi.org/10.3390/ma17215369.

[19] Csehngeri, D. *et al.* (2025). Ultrasonication accelerated curing of epoxy resin: monitoring through impedance measurement. *Nondestructive Characterization and Monitoring of Advanced Materials, Aerospace, Civil Infrastructure, and Transportation XIX*. https://doi.org/10.1117/12.3053302.

[20] Peng, Y. *et al.* (2024). Void formation and suppression in CFRP laminate using newly designed ultrasonic vibration assisted RTM technique. *Composite Structures*. https://doi.org/10.1016/j.compstruct.2023.117796.

[21] Wang, H. *et al.* (2023). Reducing Interface Defects and Porosity of Adhesive Bonded Aluminum Alloy Joints via Ultrasonic Vibration. *Polymers*. https://doi.org/10.3390/polym15092098.

[22] Wang, H. *et al.* (2021). Study on ultrasonic vibration-assisted adhesive bonding of CFRP laminates with laser ablation-treated surfaces. *Composite Structures*. https://doi.org/10.1016/j.compstruct.2021.113983.

[23] Yong, A.X.H. *et al.* (2025). Towards standardisation of the out-of-plane permeability measurement for reinforcement textiles. *Composites Part A: Applied Science and Manufacturing*. https://doi.org/10.1016/j.compositesa.2024.108630.

[24] Gerardo, C.D. *et al.* (2018). Fabrication and testing of polymer-based capacitive micromachined ultrasound transducers for medical imaging. *Microsystems & Nanoengineering*. https://doi.org/10.1038/s41378-018-0022-5.